Optical Sensing of Biomolecules Using Microring Resonators

Ayça Yalçın, *Student Member, IEEE*, Ketul C. Popat, John C. Aldridge, Tejal A. Desai, John Hryniewicz, Nabil Chbouki, Brent E. Little, Oliver King, Vien Van, Sai Chu, David Gill, Matthew Anthes-Washburn, M. Selim Ünlü, *Senior Member, IEEE*, and Bennett B. Goldberg

***Abstract*—A biosensor application of vertically coupled glass microring resonators with $Q \sim 12\,000$ is introduced. Using balanced photodetection, very high signal to noise ratios, and thus high sensitivity to refractive index changes (limit of detection of 1.8×10^{-5} refractive index units), are achieved. Ellipsometry and X-ray photoelectron spectroscopy results indicate successful modification of biosensor surfaces. Experimental data obtained separately for a bulk change of refractive index of the medium and for avidin-biotin binding on the ring surface are reported. Excellent repeatability and close-to-complete surface regeneration after binding are experimentally demonstrated.**

***Index Terms*—Biomedical transducer, cavity resonator, circular waveguide.**

I. Introduction

INTEGRATED devices featuring resonant microcavity structures such as disks, rings, toroids, and spheres have been demonstrated in add-drop filter [1], [2], optical switch [3], and laser [4], [5] applications. These devices have recently become popular for research in biological and chemical sensing [6]–[11] as the demand for compact devices to detect biomolecules has increased. Light coupled to these cavities is confined within the structure by total internal reflection, forming high quality factor (Q) resonant modes. Any interaction with the evanescent tail of the optical field affects the guided-mode, and thus changes the resonance behavior of the cavity. This change in resonance can be detected with very high sensitivity by optimizing the microcavity design and the method of observation.

In this paper, we demonstrate sensing of biomolecules using microring resonators. Their small size, low cost, and potential for high sensitivity make them attractive for biosensing applications. Fabrication of high-Q resonators is essential for achieving high sensitivity. With the Q values we report $(\sim 12\,000)$, sensitivities comparable to current devices utilizing surface plasmon resonance [12] can be reached. Microring resonator Q-values on the order of 10^6 are available, but optimizing them for sensing configurations needs to be more closely investigated. Aside from their high sensitivity, microring resonator devices are compact, integrated, and can be mass-manufactured utilizing well established silicon integrated circuit fabrication techniques.

To demonstrate sensing of biomolecules with microring resonators, the well-documented avidin-biotin binding chemistry is utilized. When a biotinylated-lectin solution is introduced to a surface previously treated with avidin, the molecular binding changes the effective index of the microcavity, and initiates a shift in its resonant modes. We report the procedure used for avidinylating the surface and verification by ellipsometry and X-ray photoelectron spectroscopy (XPS). We also describe the experimental measurement technique, and report two observations: resonance shifts induced by a change in refractive index of the medium (a bulk change) to quantify the sensitivity of the system, and resonance shifts caused by molecular binding on the surface to prove the applicability to sensing of biomolecules.

II. Vertically Coupled Microring Resonators

A. Fabrication

Microring resonator/waveguide structures have been fabricated using several materials including InGaAsP [13], Ta_2O_5/SiO_2 [14], Si_3N_4 [15], and SiON [16]. It is important to use a high refractive index contrast material to reduce bending losses. Both our microring and waveguides are fabricated through chemical vapor deposition (CVD) of a glass-based material termed Hydex,[1] which has an adjustable refractive index contrast of up to 25%.

Another critical fabrication parameter is the coupling coefficient. Coupling between the microring and the waveguides can be achieved vertically [1] or laterally [14]. The microring resonators used in this work are vertically coupled to input/output waveguides (Fig. 1). In laterally coupled structures, the input/output waveguides and the rings are all coplanar. Narrow coupling gaps are required in the lateral geometry, which taxes photolithography and results in large variations in device performance. Further, in the lateral geometry all the waveguides would be air clad and exposed to the surface treatments. In vertical coupling, the waveguides are buried and remain isolated from the effects of surface treatment. The resonator–waveguide

Manuscript received February 24, 2005; revised September 29, 2005. This work was supported in part by the Army Research Laboratory (ARL) and was accomplished under the AMCAC-RTP Cooperative Agreement DAAD19-00-2-0004. The views and conclusions contained in this document are those of the authors and should not be interpreted as representing the Laboratory or the U.S. Government. The U.S. Government is authorized to reproduce and distribute reprints for Government purposes notwithstanding any copyright notation hereon.

A. Yalçın, K. C. Popat, J. C. Aldridge, T. A. Desai, M. S. Ünlü, and B. B. Goldberg are with Boston University, Boston, MA 02215 USA (e-mail: ayca@bu.edu).

J. Hryniewicz, N. Chbouki, B. E. Little, O. King, V. Van, S. Chu, and D. Gill are with the Little Optics Division, Nomadics Inc., Annapolis Junction, MD 20701 USA (e-mail: brent_little@littleoptics.com).

M. Anthes-Washburn is with West Roxbury High School, Boston Public Schools, Boston, MA 02132 USA.

Digital Object Identifier 10.1109/JSTQE.2005.863003

[1]Little Optics Division. Nomadics Inc. Annapolis Junction, MD.

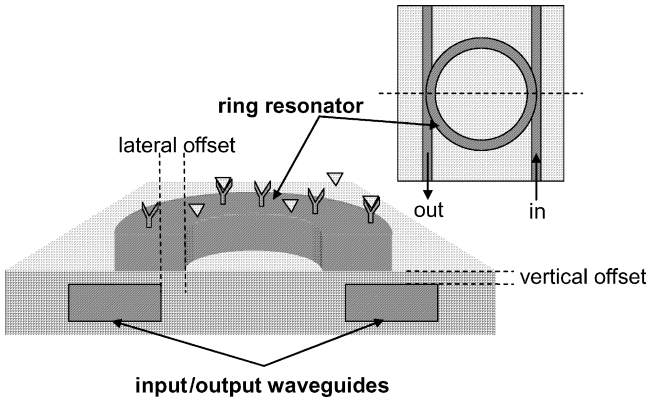

Fig. 1. Vertically coupled microring resonator and waveguides. Lateral and vertical offsets allow control over the coupling coefficient. Receptor molecules are attached to the microresonator surface, and binding occurs during flow of ligand molecules over the surface. Inset shows top view of the device.

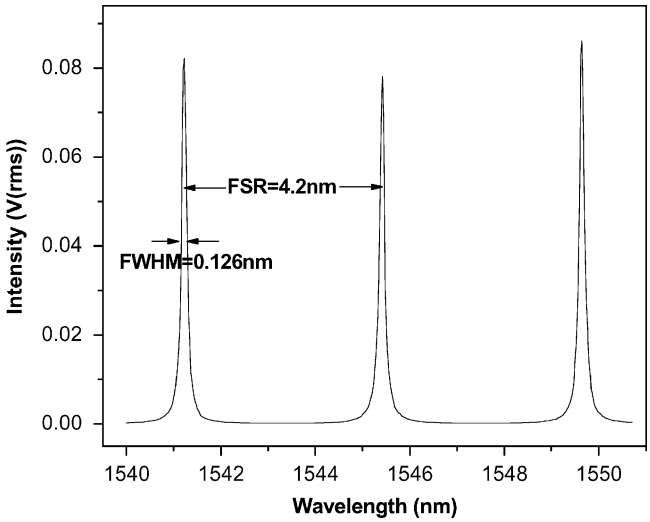

Fig. 2. Transmission spectrum of the microring coupled device for a wavelength sweep with 20-pm resolution. FSR, FWHM, Q, and F are determined from this spectrum.

separation (and, thus, the coupling coefficient) is determined by material deposition, which is a process that is much better controlled than lithography and etching [1], [15].

The microring resonator waveguide used in this experiment is monomode, with a radius of 60 μm and an effective index of $n_{\text{eff}} \approx 1.5$ measured in deionized water (DI-H_2O) ambience. The decay coefficient of the mode is given by $\alpha = (2\pi/\lambda_0)\sqrt{n_{\text{eff}}^2 - n_{\text{sol}}^2}$, where n_{sol} is the refractive index of the solution that flows over the surface. In DI-H_2O at $\lambda_0 = 1550$ nm, $\alpha \approx 28 \times 10^3$ cm^{-1} for the guided mode. This corresponds to a penetration depth of ≈ 360 nm.

B. Transmission

Fig. 2 illustrates the transmission spectrum of the microring coupled device when DI-H_2O is flowed over the surface. The peaks represent the resonant modes of this microring cavity, and their positions depend on the path length L and n_{eff} where $n_{\text{eff}}L$ is a multiple of the wavelength. Device parameters are measured from this transmission spectrum, and are reported as

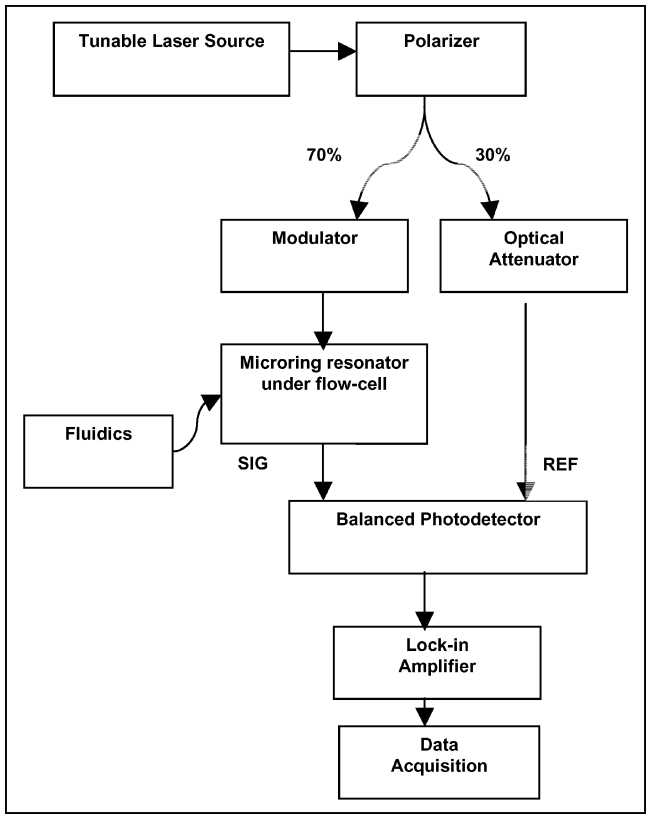

Fig. 3. Experimental setup. Microring resonator is mounted under the flow-cell.

full-width at half-maximum (FWHM) ≈ 0.126 nm, free spectral range $(\text{FSR}) = \lambda^2/Ln_{\text{eff}} \approx 4.2$ nm, $Q \sim 12\,000$, and finesse $F \approx 33$. The wavelength resolution when performing this scan was 20 pm; this step size accounts for the nominal difference in peak heights.

III. Experimental Technique

A. Setup

The experimental setup is illustrated in Fig. 3. The fiber-coupled tunable laser output is directed through a polarization controller, which is manually set for maximum signal transmission. The cavity supports both TE and TM polarization modes, and adjusting the polarizer allows one of the modes to be used. An optical splitter located after the polarizer splits the signal into two paths, with a power ratio of 70/30. The 70% arm is mechanically chopped in free space at a frequency of 220 Hz, and this modulated signal is coupled to the input waveguide of the microring. The output waveguide is coupled to a photodetector as the signal input. For balanced detection, the 30% arm is optically attenuated and connected to the photodetector as a reference input. Optical attenuation of the reference is required in order to meet the photodetector specification of reference to signal power ratio. Common-mode noise cancellation of up to 50 dB is achieved with balanced detection, effectively improving signal-to-noise ratio (SNR) and, thus, the overall system sensitivity.

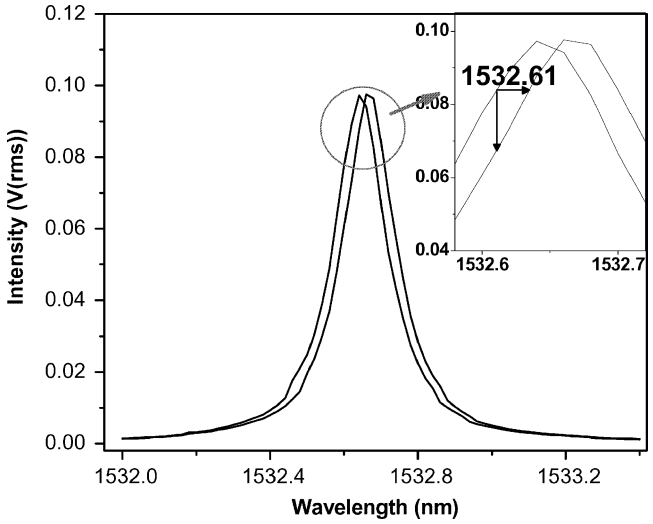

Fig. 4. A shift in resonance peak when deionized water and 0.1X PBS solution are flowed across sensor surface. The derivative of the spectrum is highest at 1532.61 nm. Inset shows the wavelength (horizontal) and intensity (vertical) shifts at this wavelength.

For phase-sensitive detection, the photodetector output signal and a reference signal from the modulator are sent to a lock-in amplifier. The filtered signal from the amplifier matches the desired frequency and phase, with noise at other frequencies rejected. This signal is acquired by LabVIEW via GPIB connection.

The microring is mounted under a custom-designed flow-cell, which facilitates the flow of solutions over the surface. Flow rate and duration are controlled by syringe pumps. A manually adjusted valve enables switching between the solutions and the elimination of air bubbles in the flow channel.

B. Data Acquisition

Fig. 4 displays an example of a shift in the resonance when DI-H_2O and 0.1X concentration of phosphate buffered saline (PBS) solution are flowed across the resonator surface. The refractive index of DI-H_2O is used as a calibration reference for a refractometer, and the difference in refractive index between DI-H_2O and 0.1X PBS is measured as $\Delta n = 1.7 \times 10^{-4}$. Direct measurement of such a shift illustrated in Fig. 4 requires repeated spectral scans to determine each new peak position. This method is time consuming, offers limited sensitivity to small refractive index changes, and much of the data collected is uninformative when determining the resonance shift [17]. Alternatively, the resonance shift can be measured indirectly by remaining at a single wavelength and observing the real-time intensity change of the signal. This signal can then be mapped to a shift in resonant modes. In terms of acquisition speed, this method is more advantageous than the first; however, it requires high optical stability. High stability is achieved by reducing the effects of laser intensity fluctuations via balanced photodetection.

To select the particular wavelength for data acquisition, the transmission spectrum is differentiated, and the wavelength corresponding to the highest derivative is selected (1532.61 nm in Fig. 4). In this way, the magnitude of the change in intensity is maximized for the smallest measurable change in refractive index.

IV. Surface Preparation

Ring resonator surfaces are modified for bulk and binding experiments using the following procedures.

A. Cleaning and Hydrophilizing Biosensor Surfaces

Surfaces were cleaned and hydrophilized using a standard RCA cleaning procedure. Surfaces were treated with 1 : 1 : 5 proportions of 30% H_2O_2, NH_4OH, and DI-H_2O at 80 °C for 10 min to remove residual metal impurities. They were subsequently washed with DI-H_2O and further treated with 1 : 1 : 6 proportions of 30% H_2O_2, 50% HCl, and DI-H_2O at 80 °C for 10 min to introduce -OH groups on the surface. The surfaces were then rinsed three times with DI-H_2O, dried with nitrogen, and used immediately for further modification.

B. Silanization

The cleaned and hydrophilized sensor surfaces were silanized with a solution phase technique. Surfaces were immersed in a 5% APTES (3-aminopropyltriethoxysilane) solution in 2-propanol for 2 h. APTES was used to silanize the silicon surfaces, since it is known to act as a bridge between biomolecules and inorganic surfaces such as silicon. The surfaces were rinsed twice with DI-H_2O to remove any weakly bonded silane on the surface. The surfaces were then dried with nitrogen and were used immediately for further avidin attachment.

C. Avidin Conjugation

Avidin conjugation was achieved using a standard EDAC (N-Ethyl-N'-(3-dimethylaminopropyl) carbodiimide hydrochloride)/NHS (N-Hydroxysuccinimide) coupling reaction [18]. A monomeric form of avidin is used in this study which allows use of mild conditions to break the avidin-biotin bonds. Silanized surfaces were immersed in a solution of 0.06M EDAC, 0.04M NHS, and 3 μM avidin in DI-H_2O at room temperature for 36 h with mild shaking at 30 r/min. Surfaces were then rinsed three times with DI-H_2 O, dried with nitrogen, and were immediately used for flow experiments.

D. Biotinylated Lectin Binding

After mounting the avidin-conjugated surface under the flow cell, a 3.5 μM solution of biotinylated lectin in DI-H_2O was flowed for 50 min at 5 μL/min. Surfaces were then rinsed three times with DI-H_2O and dried with nitrogen for surface characterization.

V. Surface Characterization

Surface characterization is performed on flat surfaces that are identical to the waveguide material. Ellipsometry and XPS measurements are taken after each step of the surface preparation protocol.

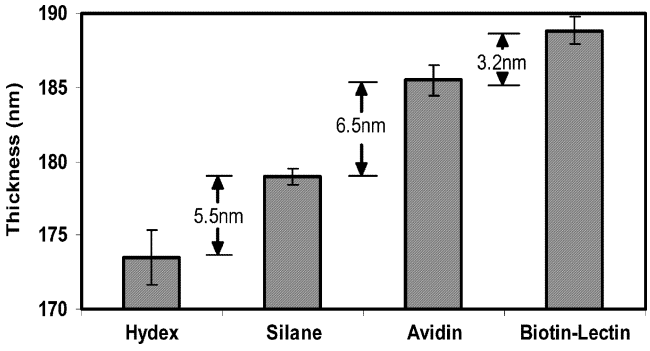

Fig. 5. Progressive increase in thickness on the original surface with modification with silane, avidin, and biotinylated lectin.

A. Spectroscopic Ellipsometry

Spectroscopic ellipsometry was used to determine surface thicknesses after each step of modification. In ellipsometry, the polarization of a light beam is altered when reflected from a bare or film-coated surface. An elliptically polarized light beam is defined by the angular position of an ellipse, its shape, and the sense of rotation of the light vector.

The states of polarization are determined by two parameters: amplitude ratio (PSI (ψ)) and phase difference (DELTA (Δ)). An automatic ellipsometer equipped with a 632.8-nm laser was used to measure thickness. Measurements were performed at a beam incidence angle of 70° at room temperature and a relative humidity of 30%–50%. Effective thicknesses were computed as the difference between the thickness of the modified and unmodified surface. Three measurements were taken on each surface to obtain average values for thickness and standard deviation.

Progressive increases in thickness from the original to final surface height provide evidence of surface deposition of successive molecular layers. The baseline thickness of the unmodified hydrophilized surfaces was normalized to 0 nm to account for the presence of native oxide. The silane layer thickness after APTES modification was approximately 5.5 nm (Fig. 5). Based on this measurement, it is likely that APTES chains not only attached to surface -OH groups but also oligomerized to form multiple silane layers. Avidin conjugation increased the surface height by 6.5 nm, and binding of biotinylated lectin added an additional 3.2-nm-thick layer to the surface (Fig. 5). These ellipsometer measurements show that surface thicknesses increased after silanization, avidin conjugation, and biotinylated lectin conjugation, suggesting successful deposition of discrete layers on the surface.

B. X-Ray Photoelectron Spectroscopy (XPS)

XPS analysis was performed to determine the chemical composition of unmodified, silane-, avidin-, and biotinylated lectin-immobilized surfaces. An x-ray photoelectron spectrometer with a monochromatic Al-$K\alpha$-X-ray small spot source (1486.6 eV) and multichannel detector was used for this analysis. A concentric hemispherical analyzer (CHA) was operated in constant analyzer transmission mode to measure the binding energies of emitted photoelectrons. The binding energy scale was calibrated

TABLE I
C/Si AND N/Si RATIOS FOR VARIOUS SURFACES OBTAINED FROM ATOMIC SURFACE CONCENTRATIONS COMPUTED USING SURVEY SCANS

	C/Si	N/Si
Hydex	0.25	0
Silane	0.86	0.88
Avidin	0.96	0.97
Biotinylated Lectin	1.33	1.04

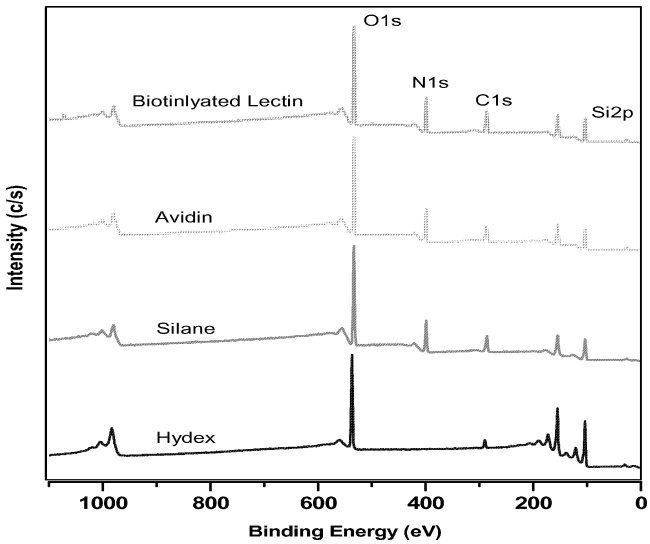

Fig. 6. XPS survey scans for various surfaces showing overall elemental constituents.

by the Au4$f_{7/2}$ peak at 83.9 eV, and the linearity was verified by the Cu3$p_{1/2}$ and Cu2$p_{3/2}$ peaks at 76.5 and 932.5 eV, respectively. Survey spectra were collected from 0 to 1100 eV with pass energy of 160 eV, and high-resolution spectra were collected for the C1s peak with pass energy of 10 eV. All spectra were referenced by setting the C1s peak to 285.2 eV to compensate for residual charging effects. Data for percent atomic composition and atomic ratios were calculated using analysis software. For peak fit analysis, a convolution of Gaussian components was assumed for all peak shapes.

Table I shows the ratios of atomic compositions of C/Si and N/Si for different surfaces obtained from XPS survey scans (Fig. 6). The data shows that surface carbon increased after modification with silane and subsequent immobilization of avidin and biotinylated lectin (carbon on hydex due to impurities). These increases were expected since APTES, avidin, and biotinylated lectin are composed predominantly of carbon.

Cleaned and hydrophilized surfaces lacked nitrogen, while silanized surfaces with APTES contained nitrogen. With subsequent surface immobilization of avidin and biotinylated lectin, the N/Si ratios increased as a result of amide groups in avidin and biotin. The silicon percentage decreased after each surface

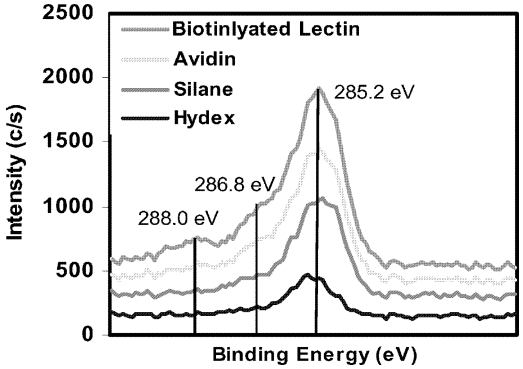

Fig. 7. High-resolution C1s scans for various surfaces showing different carbon chemistries.

TABLE II
RESULTS OF DECONVOLUTION OF HIGH-RESOLUTION C1S SPECTRA INTO FRACTIONS OF VARIOUS PEAKS REPRESENTING DIFFERENT CARBON CHEMISTRIES

	C-C (285.0eV)	CH_2N/CH_2O (286.8eV)	O=C-N (288.0eV)
Hydex	1	0	0
Silane	0.795	0.205	0
Avidin	0.559	0.227	0.214
Biotinylated Lectin	0.485	0.273	0.242

layer deposition, as expected since XPS is a depth sensitive technique. Because XPS characterizes only the uppermost (7–10 nm) surface chemistries, bulk silicon is masked as more layers are deposited.

To further support the presence of APTES, avidin, and biotinylated lectin on the surface after modification, high resolution C1s scans were taken (Fig. 7). The major hydrocarbon peak (C-C) is at 285.2 eV. The binding energy at 286.8 eV is assigned to amines (CH_2N) and alkoxy groups (CH_2-O), and the binding energy at 288.0 eV is assigned to amide functional groups (O=C-N).

For the APTES modified surface, a peak at 286.8 eV is seen, which confirms the covalent attachment of the aminosilane on the surface. After avidin attachment, the peak at 286.8 eV increases and a peak at 288.0 eV appears. Furthermore, an increase in these peaks after biotinylated lectin conjugation supports the presence of biotinylated lectin on the surface.

Table II shows the deconvolution of high resolution C1s spectra into separate peaks. The decrease in the peak at 285.2 eV and the subsequent increase in peaks at other binding energies reflect the successful modification of the surfaces with silane, avidin, and biotinylated lectin.

VI. RESULTS AND ANALYSIS

A. Bulk Experiments

Cleaned and hydrophilized surfaces (without avidin) were used for bulk flow experiments. DI-H_2O and degrading concentrations of PBS were flowed consecutively across the resonator surface, and the signal at a single wavelength is recorded in real-time (Fig. 8). In the figure, the inset shows the instants when PBS and DI-H_2O are introduced to the flow cell. Each PBS concentration cycle is applied three times to demonstrate repeatability.

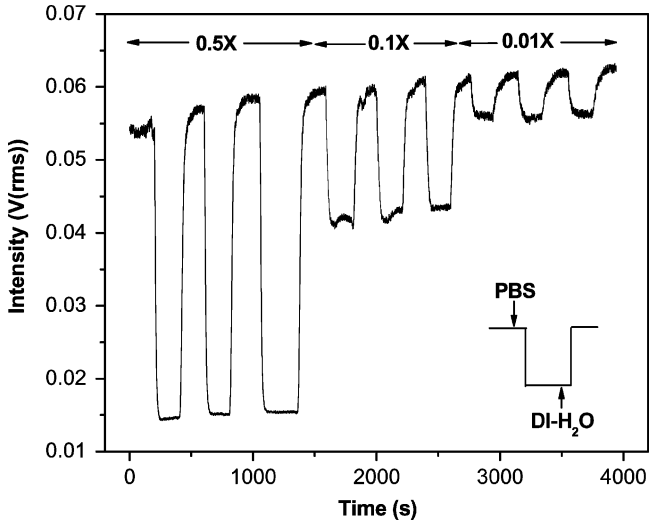

Fig. 8. A real-time recording of the change in intensity as 0.5X, 0.1X, and 0.01X PBS concentrations are introduced. Each concentration is flowed for three consecutive cycles.

As shown in Fig. 8, the signal level is stable within a single PBS concentration flow, and the difference between the DI-H_2O and PBS signal level (corresponding to upper and lower levels respectively) decreases with decreasing concentration. To obtain the relation between the PBS concentration (or the refractive index of the medium) and the shift in resonance, the change in signal level (ΔT) in each cycle is measured using a linear curve fit. By differentiating the transmission spectrum (λ versus T) that is recorded in each cycle before introducing PBS, the shift in resonance $(\Delta\lambda)$ can be determined using $(d\lambda/dT)\Delta T = \Delta\lambda$ The resulting relationship between the refractive index of the flowed solution and the corresponding resonance shift is plotted in Fig. 9, which shows a strong linear fit.

To approximate the limit of detection, $\mathrm{LOD}(n)$, for a change in refractive index, we calculated the standard deviations, δ (pm), of the signal levels during PBS flow. According to $\mathrm{LOD}(n) = 3\delta/m$, where m is the slope of the curve in Fig. 9, $\mathrm{LOD}(n)$ is calculated to be 1.8×10^{-5} refractive index units (RIU).

B. Binding Experiments

After calculating an approximate value for the refractive index sensitivity of our system, we turned our attention to binding experiments, where resonant mode shifts are caused by binding of molecules on the surface. Avidin–biotin interaction is selected because of its well known bond strength approaching that of a covalent bond with an affinity constant of 10^{-15} Molar. The experiment consists of two parts: binding and regeneration. In the binding portion, a 3.5 μM biotinylated lectin solution is

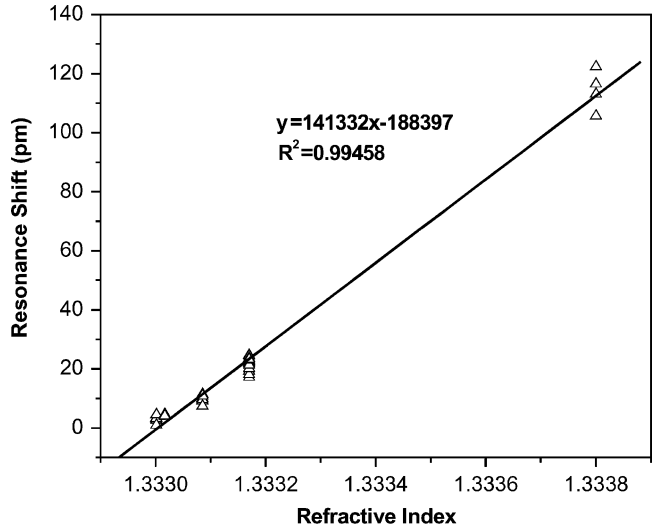

Fig. 9. Linear relation between refractive index and the resonance shift. The slope is used to determine the limit of detection for refractive index.

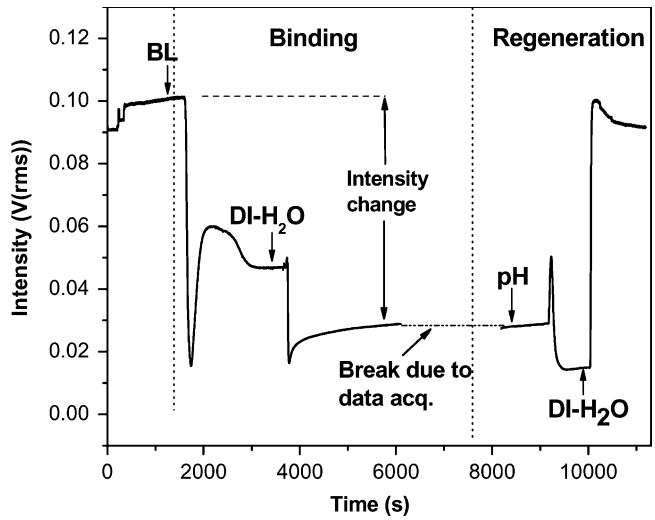

Fig. 10. Data from binding experiment illustrating binding and regeneration phases. (BL: biotinylated lectin, DI-H_2O: deionized water, pH: pH-7 buffer). Binding efficacy is measured between the signal levels when DI-H_2O is flowed.

flowed over the surface. The biotin molecules bind to the avidin molecules attached to the surface, and a new signal level is reached. Once the signal level is stabilized, DI-H_2O is flowed to wash away any unbound biotinylated lectin, and to bring the bulk refractive index of the medium to the same prebinding level. For surface regeneration, a chemical pH-7 buffer is introduced to break the avidin-biotin bonds, and is followed by a DI-H_2O flow.

The real-time intensity recording is shown in Fig. 10, where binding and regeneration phases can be distinguished. The change in transmission is not governed by an approximate step function anymore (as it was in bulk experiments), but is now dependent on the binding kinetics of the avidin-biotin complex.

As shown in Fig. 10, the actual amount of change in the signal due to binding is measured between the DI-H_2O flow levels before and after the introduction of biotinylated lectin to the system. At these two levels, the solution running across the surface is identical, and thus the change in intensity is caused only by binding of molecules on the surface. The signal level reached when the regeneration phase is complete indicates that avidin-biotin bonds are broken and close to complete regeneration of the surface is achieved.

As a control experiment, a biotinylated lectin solution of the same concentration was flowed over a surface on which no avidin-conjugation had been performed. The intensity recording from this experiment shows the same step function-like behavior as the bulk experiments with PBS. As in the bulk experiments, there is no appreciable difference between DI-H_2O signal levels before and after biotinylated lectin flow. This indicates that biotinylated lectin did not bind to the surface, and the flow of DI-H_2O removed all the biotinylated lectin molecules from the medium. Furthermore, the difference between the signal levels of biotinylated lectin and DI-H_2O flow is much smaller in magnitude compared to those for the binding experiments, because they correspond only to a bulk change in refractive index, rather than strong binding of molecules to the surface. These observations strengthen our claim that the binding experiments demonstrate specific binding of biotin to surface-bound avidin.

VII. Conclusion

A surface preparation protocol to modify the surfaces for binding experiments, and an experimental measurement technique, are reported. Surface characterization by ellipsometry and XPS revealed both successful deposition of biolayers on the surface, and binding of biotin to surface-bound avidin. Bulk experiments showed a linear relationship between the refractive index change of the surrounding medium and the resonance shift. The refractive index sensitivity of the system is found to be 1.8×10^{-5}. Comparison of data from control and binding experiments indicate the system's capability to measure specific avidin-biotin binding.

Acknowledgment

The authors would like to thank Dr. G. Ulu, D. A. Rodriguez, and A. Ying for their contributions.

References

[1] B. E. Little, S. T. Chu, W. Pan, D. Ripin, T. Kaneko, Y. Kokubun, and E. P. Ippen, "Vertically coupled glass microring resonator channel dropping filters," *IEEE Photon. Technol. Lett.*, vol. 11, no. 2, pp. 215–217, Feb. 1999.

[2] M. Cai, G. Hunziker, and K. Vahala, "Fiber optic add-drop device based on a silica microsphere-whispering gallery mode system," *IEEE Photon. Technol. Lett.*, vol. 11, no. 6, pp. 686–687, Jun. 1999.

[3] V. Van, T. A. Ibrahim, K. Ritter, P. P. Absil, F. G. Johnson, R. Grover, J. Goldhar, and P.-T. Ho, "All-optical nonlinear switching in GaAs-AlGaAs microring resonators," *IEEE Photon. Technol. Lett.*, vol. 14, no. 1, pp. 74–76, Jan. 2002.

[4] L. Yang, D. K. Armani, and K. J. Vahala, "Fiber-coupled erbium microlasers on a chip," *Appl. Phys. Lett.*, vol. 83, no. 5, pp. 825–826, Aug. 2003.

[5] B. Liu, A. Shakouri, and J. E. Bowers, "Passive microring-resonator-coupled lasers," *Appl. Phys. Lett.*, vol. 79, no. 22, pp. 3561–3563, Nov. 2001.

[6] K. J. Vahala, "Optical microcavities," *Nature*, vol. 424, pp. 839–846, Aug. 2003.
[7] R. W. Boyd and J. E. Heebner, "Sensitive disk resonator photonic biosensor," *Appl. Optics*, vol. 40, no. 31, pp. 5742–5747, Nov. 2001.
[8] S. Arnold, M. Khoshsima, I. Teraoka, S. Holler, and F. Vollmer, "Shift of whispering-gallery modes in microspheres by protein adsorption," *Opt. Lett.*, vol. 28, no. 4, pp. 272–274, Feb. 2003.
[9] F. Vollmer, D. Braun, A. Libchaber, M. Khoshsima, I. Teraoka, and S. Arnold, "Protein detection by optical shift of a resonant microcavity," *Appl. Phys. Lett.*, vol. 80, no. 21, pp. 4057–4059, May 2002.
[10] A. Serpenguzel, S. Isci, T. Bilici, and A. Kurt, "Microsphere-based optical system for biosensor applications," in *Proc. SPIE-Int. Soc. Opt. Eng. Optical Fibers and Sensors for Medical Applications IV*, Jun. 2004, vol. 5317, pp. 180–185.
[11] J. Hryniewicz, N. Chbouki, B. E. Little, O. King, V. Van, S. Chu, and D. Gill, "Microring resonators: The promise of a powerful biochemical sensor platform," in *Biophotonics/Optical Interconnects and VLSI Photonics/WBM Microcavities, 2004 Dig. LEOS Summer Topical Meetings*, Jun. 2004, pp. 33–34.
[12] F. Bardin, I. Kasik, A. Trouillet, V. Matejec, H. Gagnaire, and M. Chomat, "Surface plasmon resonance sensor using an optical fiber with an inverted graded-index profile," *Appl. Opt.*, vol. 41, no. 13, pp. 2514–2520, May 2002.
[13] S. J. Choi, K. Djordjev, Z. Peng, Q. Yang, S. J. Choi, and P. D. Dapkus, "Laterally coupled buried heterostructure high-Q ring resonators," *IEEE Photon. Technol. Lett.*, vol. 16, no. 10, pp. 2266–2268, Oct. 2004.
[14] G. H. V. Rhodes, B. B. Goldberg, M. S. Unlu, S. T. Chu, and B. E. Little, "Internal spatial modes in glass microring resonators," *IEEE J. Sel. Topics Quantum Electron.*, vol. 6, no. 1, pp. 46–53, Jan./Feb. 2000.
[15] J. Guo, M. J. Shaw, G. A. Vawter, P. Esherick, G. R. Hadley, and C. T. Sullivan, "High-Q integrated on-chip micro-ring resonator," in *Proc. 17th Annu. Meeting IEEE/LEOS*, vol. 2, Nov. 2004, pp. 745–746.
[16] F. S. Tan, H. Kelderman, and A. Driessen, "Bandpass filter based on parallel cascaded multiple microring resonators," in *Proc. AIP Conf.*, vol. 709, no. 1, May 2004, pp. 417–418.
[17] L. J. Guo, C. Y. Chao, W. Fung, and J. Yang, "Biochemical sensors based on polymer microring resonators," in *Proc. SPIE-Int. Soc. Opt. Eng.*, Oct. 2004, vol. 5517, pp. 152–162.
[18] S. L. Tao, M. W. Lubeley, and T. A. Desai, "Bioadhesive poly(methyl methacrylate) microdevices for controlled drug delivery," *J. Controlled Release*, vol. 88, pp. 215–228, 2003.

Ayça Yalçın (S'04) was born in Istanbul, Turkey, in 1982. She received the B.S. degree in electrical and electronics engineering from Bilkent University, Ankara, Turkey, in 2003, and the M.S. degree in photonics from Boston University, Boston, MA, in 2005. She is currently working toward the Ph.D. degree in electrical and computer engineering at Boston University, Boston, MA.

Ms. Yalçın is a member of the American Physical Society (APS).

Ketul C. Popat received the B.S. degree in chemical engineering from M.S. University, India, in 1998, the M.S. degree in chemical engineering from the Illinois Institute of Technology, Chicago, in 2000, and the Ph.D. degree in bioengineering from the University of Illinois, Chicago, in 2002.

Currently, he is a Senior Research Associate in the Therapeutic Micro/Nanotechnology Laboratory directed by Dr. T. A. Desai at Boston University, Boston, MA. His current research includes biomaterials, micro/nanotechnology, and tissue engineering. He has authored over ten peer-reviewed publications in journals, and has presented his work at numerous national and international conferences.

John C. Aldridge received the B.S. degree in optical engineering from the University of Arizona, Tucson, in 2002, and is currently working toward the M.S. degree in photonics at Boston University, Boston, MA, as a participant in MIT Lincoln Laboratory's Lincoln Scholars Program.

As an undergraduate, he interned at Innovative Lasers Corporation, Tucson, AZ, in 1999, and the Data Storage Institute, Singapore, in 2000. Since 2002, he has held the position of Assistant Staff at MIT Lincoln Laboratory, Lexington, MA.

Mr. Aldridge is a member of the American Physical Society (APS).

Tejal A. Desai received the B.Sc. degree in biomedical engineering from Brown University, Providence, RI, in 1994, and the Ph.D. degree in bioengineering from the joint graduate program at the University of California, Berkeley, and the University of California, San Francisco, in 1998.

In September 1998, she was appointed an Assistant Professor in the newly formed Department of Bioengineering at the University of Illinois, Chicago. In January 2002, she joined the Biomedical Engineering faculty at Boston University, Boston, MA, as an Associate Professor. She directs the Laboratory of Therapeutic Micro and Nanotechnology. In addition to authoring over 60 technical papers, she is presently serving on the editorial boards of *Langmuir, Biomedical Microdevices*, and *Sensor Letters*, and is editing a book on therapeutic microtechnology. She has chaired and organized several conferences and symposia.

Dr. Desai has earned her numerous awards through her research efforts. In 1999, she was recognized by *Crain's Chicago Business* magazine with their annual "40 Under 40" award for leadership. She was also named that year by *Technology Review Magazine* as one of the nation's "Top 100 Young Innovators" and *Popular Science*'s Brilliant 10. She won the College of Engineering Best Advisor/Teacher Award, India, New England's Woman of the Year, the National Science Foundation's "New Century Scholar" award, the NSF Faculty Early Career Development Program "CAREER" award, the Visionary Science Award from the International Society of BioMEMS and Nanotechnology, and the 2003 Eurand Award.

John Hryniewicz, photograph and biography not available at the time of publication.

Nabil Chbouki, photograph and biography not available at the time of publication.

Brent E. Little, photograph and biography not available at the time of publication.

Oliver King, photograph and biography not available at the time of publication.

Vien Van, photograph and biography not available at the time of publication.

Sai Chu, photograph and biography not available at the time of publication.

David Gill, photograph and biography not available at the time of publication.

Matthew Anthes-Washburn, photograph and biography not available at the time of publication.

M. Selim Ünlü (S'90–M'92–SM'95) received the B.S. degree from Middle East Technical University, Ankara, Turkey, in 1986, and the M.S.E.E. and Ph.D. degrees from the University of Illinois, Urbana-Champaign, in 1988 and 1992, respectively, all in electrical engineering.

In 1992, he joined the Department of Electrical and Computer Engineering, Boston University, Boston, MA. He was a Visiting Professor at the University of Ulm, Ulm, Germany, in 2000. He is a Professor of Electrical and Computer Engineering, Biomedical Engineering, and Physics at Boston University. He is also serving as the Associate Chair of ECE for graduate studies and the Associate Director of the Center for Nanoscience and Nanobiotechnology. He has authored or coauthored over 200 technical articles and several book chapters and magazine articles; edited one book; and holds several patents. His interests include photonic materials, devices, and systems focusing on the design, processing, characterization, and modeling of semiconductor optoelectronic devices, especially photodetectors, as well as high-resolution microscopy and spectroscopy of semiconductor and biological materials.

Dr. Ünlü served as the Chair of IEEE Lasers and Electro-Optics Society, Boston Chapter, during 1994–1995, winning the LEOS Chapter-of-the-Year Award. He was awarded the National Science Foundation Research Initiation Award in 1993, United Nations TOKTEN award in 1995 and 1996, and both the National Science Foundation CAREER and Office of Naval Research Young Investigator Awards in 1996. He served as Chair of the IEEE/LEOS Technical Subcommittee on photodetectors and imaging, and the nano-optics committees for CLEO/QELS and IQEC. He is currently an Associate Editor for the IEEE JOURNAL OF QUANTUM ELECTRONICS.

Bennett B. Goldberg was born in Boston, MA, in 1959. He received the B.A. degree from Harvard College, Cambridge, MA, in 1982, and the M.S. and Ph.D. degrees in physics from Brown University, Providence, RI, in 1984 and 1987, respectively.

Following a Bantrell postdoctoral appointment at the Massachusetts Institute of Technology and the Francis Bitter National Magnet Lab, he joined the physics faculty at Boston University, Boston, MA, in 1989, where his is now a Professor of Physics, Professor of Electrical and Computer Engineering, and Professor of Biomedical Engineering. He is currently Chair of the Physics Department, and his active research interests are in the general area of ultra-high-resolution microscopy and spectroscopy techniques for hard and soft material systems. He has worked in near-field imaging of photonic bandgap, ring microcavity, and single-mode waveguide devices, and has recently developed subsurface solid immersion microscopy for Si inspection. His group is working on novel approaches to subcellular imaging with interferometric fluorescenent techniques, and in biosensor fabrication and development of waveguide evanescent bio-imaging techniques. Nano-optics research includes Raman scattering of individual nanotubes and nano-optics of electron systems in quantum wells and quantum dot structures. He is Director of Boston University's new Center for Nanoscience and Nanobiotechnology, an interdisciplinary center that brings together academic and industrial scientists and engineers in the development of nanotechnology with applications in materials and biomedicine.

Prof. Goldberg has been a member of the American Physical Society, MRS, and the IEEE Lasers and Electro-Optics Society.